Effects of p-GaN Body Doping Concentration on the ON-State Performance of Vertical GaN Trench MOSFETs

Renqiang Zhu, *Graduate Student Member, IEEE*, Huaxing Jiang, *Member, IEEE*, Chak Wah Tang, and Kei May Lau, *Life Fellow, IEEE*

***Abstract*— In this letter, we report the influence of p-GaN body doping concentration on the ON-state performance of vertical GaN trench MOSFETs. Decreasing the p-GaN body doping concentration leads to an enhanced maximum drain current ($I_{D,max}$), reduced specific ON-resistance ($R_{ON,sp}$), but also a decreased threshold voltage (V_{th}), suggesting that the p-GaN doping plays an important role in balancing the V_{th}, $R_{ON,sp}$ and $I_{D,max}$ in vertical GaN trench MOSFETs. Resulting from the tuning of Mg concentration in the p-GaN, we demonstrate high ON-performance including a high $I_{D,max}$ of 2.8 kA/cm^2, a low $R_{ON,sp}$ of 0.87 mΩ·cm^2, a large V_{th} of 4.8 V in a quasi-vertical GaN trench MOSFET on sapphire with a 2.5-μm-thick drift layer, while maintaining a breakdown voltage of 273 V.**

***Index Terms*— Gallium nitride, vertical trench MOSFET, channel doping, ON-state performance.**

I. Introduction

ALGAN/GAN based lateral GaN power transistors have demonstrated great promise for low and medium voltage ($\leq$ 650 V) power switching applications over the past decade [1]–[5]. To enhance the voltage rating and current handling capability of GaN transistors, device structures with vertical current conduction path have attracted extensive research interest [6]–[20]. Current aperture vertical electron transistors (CAVETs) [14], [16], [17], vertical fin MOSFETs [19], [20], and inversion channel vertical trench MOSFETs [6], [7] with a high breakdown voltage over 1 kV have been achieved. On the other hand, low ON-resistance (R_{ON}) to minimize the power loss, high output current (I_{ON}) to maximize the driving capability, and large threshold voltage (V_{th}) (>3 V) to avoid false turn-on are always highly desired device metrics in these devices.

However, among the above mentioned three types of vertical GaN transistors, the CAVETs and vertical FinFETs were mainly operated in accumulation-mode, usually resulting in a small V_{th} (typically ~1-2 V). Their fabrication processes were also relatively complicated (channel regrowth or precise dry etch required), which may slow down their pace for wide adoption in manufacturing. As for the vertical GaN trench MOSFETs, despite the remarkable progress made in recent years [6]–[12], the ON-state performance including the R_{ON} and $I_{D,max}$ are not on par with the CAVET [12]–[17] and their vertical fin MOSFET [18]–[20] counterparts, mainly because of the large channel resistance of the inversion channel layer in the trench MOSFETs. To take advantage of the simple device fabrication process and resulting large V_{th} of GaN trench MOSFETs, lowering the channel resistance-dominated R_{ON} is essential to minimize the total power loss of the device. Although the ON-state performance of vertical trench MOSFETs was improved by optimizing the gate trench formation process [11], [21]–[23], the impact of material parameters, especially the body doping, of the device epilayers, has seldom been reported.

In this work, we investigated the effects of p-GaN body doping concentration on the ON-state performance of vertical GaN trench MOSFETs. We found that decreased p-GaN body doping concentration results in enhanced $I_{D,max}$, reduced $R_{ON,sp}$, but a lower V_{th}. Resulting from the fine tuning of the Mg doping concentration in the channel layer, a high ON-performance quasi-vertical GaN trench MOSFET is demonstrated, exhibiting not only a large V_{th} of 4.8 V, but also an ultralow specific on-resistance ($R_{ON,sp}$) of 0.87 mΩ·cm^2 in conjunction with a high $I_{D,max}$ of 2.8 kA/cm^2.

II. Device Design and Fabrication

The n^+-p-n^--n^+-GaN structures for the quasi-vertical trench MOSFETs were grown on sapphire substrates by MOCVD (Fig. 1). The epilayers, from bottom to top, consist of a 1-μm i-GaN buffer, a 1-μm n^+-GaN [Si: 5×10^{18} cm^{-3}], a 2.5-μm n^--GaN drift layer [Si: 5×10^{16} cm^{-3}], a 400-nm p-GaN body (Mg-doped), and a 200-nm n^+-GaN layer [Si: 5×10^{18} cm^{-3}]. Five samples (denoted as sample A, B, C, D, and E) were grown with the same structure and growth conditions except for the Mg doping concentration in the p-GaN body. The Mg concentration was varied from 3.0 to 1.2 $\times10^{19}$ cm^{-3}, as confirmed by secondary-ion mass spectrometry (SIMS) depth-profiling measurements (Fig. 1(b)).

All the samples shared the same fabrication procedures. The device process started with Cl_2/BCl_3-based dry etching of the gate trench (~900 nm-deep) with a Ni hard mask, followed by hot tetramethylammonium hydroxide (TMAH) wet etching to remove the dry etching induced damage in the gate trenches [21], [24]. The gate trench sidewalls were aligned to the *m*-plane for better ON-state performance [11], [22]. Process continued with the mesa formation and exposure of bottom n^+-GaN layer for drain Ohmic contacts. After the

Manuscript received April 1, 2021; revised April 27, 2021; accepted May 11, 2021. Date of publication May 14, 2021; date of current version June 29, 2021. This work was supported by the Research Grants Council of Hong Kong under General Research Fund Grant 16215818. The review of this letter was arranged by Editor Y. Wu. *(Corresponding authors: Huaxing Jiang; Kei May Lau.)*

The authors are with the Department of Electronic and Computer Engineering, The Hong Kong University of Science and Technology, Hong Kong (e-mail: hjiangab@connect.ust.hk; eekmlau@ust.hk).

Color versions of one or more figures in this letter are available at https://doi.org/10.1109/LED.2021.3080260.

Digital Object Identifier 10.1109/LED.2021.3080260

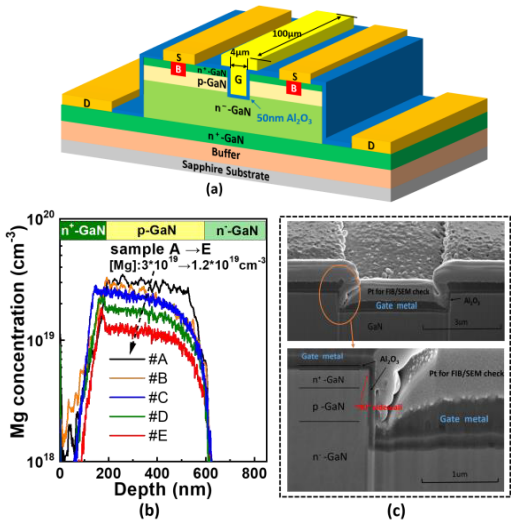

Fig. 1. (a) 3-D cross-sectional schematic of fabricated quasi-vertical GaN trench MOSFETs. (b) Secondary ion mass spectrometry (SIMS) depth-profiling results of Mg concentration in the p-GaN layer of different samples. (c) Cross-sectional SEM images of the gate trench region of a fabricated device.

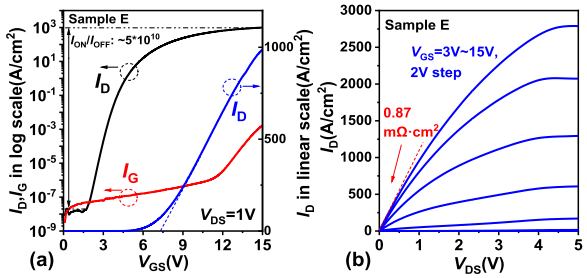

Fig. 2. (a) Transfer and (b) output curves of sample E.

p-GaN body contact was opened, the buried p-GaN body was then activated via rapid thermal annealing at 800°C for 10 min in an N_2 ambient. Subsequently, a 50-nm Al_2O_3 gate dielectric was deposited by atomic layer deposition (ALD). After removing the gate oxide in the body, source/drain contact regions, the p-body contact with a Ni/Au metal stack was deposited and annealed, followed by the Ti/Al/Ni/Au metal stack for the source and drain Ohmic contact. Finally, a Ti/Al metal stack was sputtered as the gate contact. It was noted that the p-GaN body contact is non-ideal Ohmic contact with a turn-on voltage of around 3 V, due to the dry-etching induced damage to the p-GaN surface [25], [26].

Fig. 1(c) shows the cross-sectional SEM images of the gate region in a fabricated device. Near 90-degree vertical sidewalls of the gate trench can be observed, which has been reported vital for the carrier transport [11]. The devices reported here feature a rectangular gate trench with a 4 μm×100 μm area. The active area (A) of the device for specific ON-resistance and current density normalization is regarded as (4 μm trench length +2.5 μm drift region thickness) × (100 μm trench width +2.5 μm drift region thickness) = 666.25 μm^2, taking the lateral current spreading length (2.5 μm) in the drift region into account [10]–[13].

III. Device Results and Discussion

Fig. 2 plots the transfer and output characteristics of a device on sample E (lowest Mg concentration among the five samples) that shows the best overall ON-state performance with the lowest $R_{ON,sp}$, the highest $I_{D,max}$, and a large V_{th}.

TABLE I
Summary of Mg Concentration of p-GaN From SIMS and Corresponding On-State Device Parameters (Average Value Measured From Ten Devices on Each Sample) for Different Samples

Sample	A	B	C	D	E
Mg concentration of p-GaN (10^{19} cm^{-3})	3.0	2.6	2.3	1.8	1.2
V_{th} (V) @1 A/cm^2	7.75	7.53	7.05	5.21	4.70
$I_{D,max}$ (A/cm^2)	400	635	713	1261	2605
$R_{ON,sp}$ (mΩ·cm^2)	4.83	2.95	2.39	1.66	0.89
V_{th} hysteresis (V)	1.33	1.36	1.28	1.30	1.26
$\Delta V_{th}/\Delta V_{DS}$ (mV/V)	93	91	98	107	105

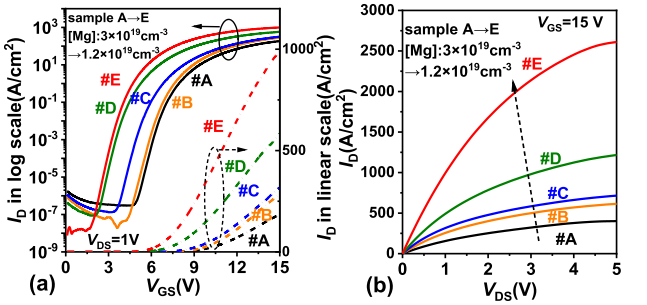

Fig. 3. (a) $I_D - V_{GS}$(at V_{DS} = 1 V) and (b) $I_D - V_{DS}$ (at V_{GS} = 15 V) curves of the five samples with different Mg concentrations of p-GaN.

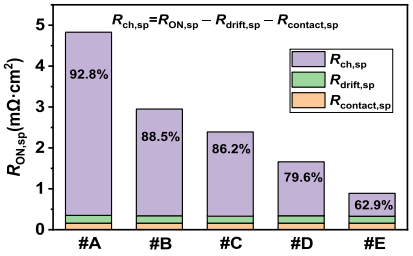

Fig. 4. $R_{ON,sp}$ breakdown of devices on the five samples with varied Mg concentration in p-GaN body. The percentages of $R_{ch,sp}$ to total $R_{ON,sp}$ on five samples are labeled.

At V_{DS} =1 V, an ultrahigh ON/OFF current ratio of ~5×10^{10}, a large V_{th} of 4.8 V at I_D of 1 A/cm^2(7.4 V from linear extrapolation), a reasonable subthreshold slope of 280 mV/dec, and a low gate current of 1.7 × 10^{-3}A/cm^2 at V_{GS} of 15 V are achieved in the device (Fig. 2(a)). The gate leakage can be further reduced by optimizing the dry etching and gate dielectric deposition conditions. In addition, a high $I_{D,max}$ of 2.8 kA/cm^2 and a low $R_{ON,sp}$ of 0.87 mΩ·cm^2 are also demonstrated (Fig. 2(b)). The V_{th} measured at V_{DS} =10 V is negatively shifted to 3.9 V at I_D of 1 A/cm^2, resulting in a drain-bias-induced V_{th} shift ($\Delta V_{th}/\Delta V_{DS}$) of ~100 mV/V. The reason behind the drain-bias-induced V_{th} shift is under investigation.

Fig. 3 compares the representative I_D-V_{GS} (at V_{DS} = 1 V) and I_D-V_{DS} (at V_{GS} = 15 V) curves of the five samples, with key device parameters (V_{th}, $I_{D,max}$, $R_{ON,sp}$, V_{th} hysteresis from I_D-V_{GS} double sweep, and drain-bias-induced V_{th} shift ($\Delta V_{th}/\Delta V_{DS}$)) summarized in TABLE I. From sample A to E, the average $R_{ON,sp}$ decreases from 4.83 to 0.89 mΩ·cm^2, corresponding to the dramatic increase of the $I_{D,max}$ from 400 to 2605 A/cm^2. Fig. 4 shows the contributions of the total $R_{ON,sp}$ of the five samples, consisting of contact resistance ($R_{contact,sp}$,

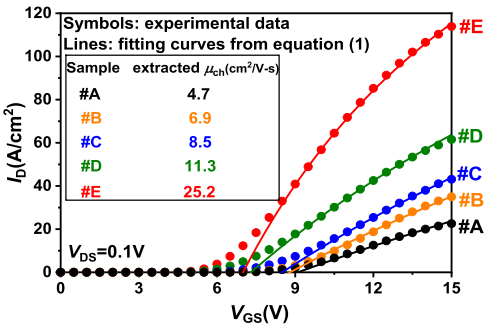

Fig. 5. Comparison of inversion channel mobility of devices on the five samples with varied Mg concentrations in p-GaN body.

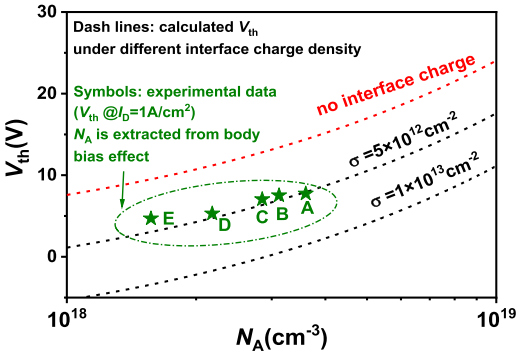

Fig. 6. Experimental V_{th} and calculated V_{th} with/without interface charge as a function of N_A.

including S/D contact layers and Ohmic contacts resistance), drift layer resistance ($R_{drift,sp}$) and channel resistance ($R_{ch,sp}$). The $R_{contacts,sp}$ is calculated based on the transmission line measurement (TLM) of the top and bottom n^+-GaN layers on each sample. The $R_{drift,sp}$ is estimated based on Schottky diodes with the same drift layer. The $R_{ch,sp}$ is calculated by $R_{ch,sp} = R_{ON,sp} - R_{drift,sp} - R_{contact,sp}$. Since the five samples show nearly identical $R_{drift,sp}$ (~0.16 mΩ·cm^2) and $R_{contact,sp}$ (~0.18 mΩ·cm^2), the drastic drop in $R_{ON,sp}$ mainly resulted from the reduction of the $R_{ch,sp}$ with the decrease of Mg concentration in the p-GaN body can be inferred.

To further correlate the ON-state channel resistance with the body doping concentration, the electron mobility (μ_{ch}) of the inversion channel of each sample is extracted by fitting the equation [27]:

$$I_D = \frac{V_{DS}}{\frac{A}{\frac{W}{L}u_{ch}C_{ox}(V_{GS}-V_{th})} + R_{drift,sp} + R_{contact,sp}}, (V_{GS} > V_{th}) \quad (1)$$

with measured I_D-V_{GS} curves (Fig. 5) at V_{DS} of 0.1 V, considering the series resistance from the drift and contact layers. In (1), A is the active area of 666.25 μm^2, W is the gate width of 208 μm, L is the gate length of 0.4 μm, and C_{ox} is the gate oxide capacitance per unit area. We observe an increasing trend of inversion channel mobility with the decrease of Mg concentration, from 4.7 cm^2/V-s for sample A to 25.2 cm^2/V-s for sample E. With a lower Mg concentration in the p-GaN body, the impurity scattering is reduced for the electrons in the inversion channel thus increasing the carrier mobility [28].

On the other hand, from sample A to E, the average V_{th} (defined at I_D of 1 A/cm^2) decreases from 7.75 V to 4.70 V, following the decrease of acceptor concentration in the body as expected. Therefore, the reduction of $R_{ON,sp}$ at the same maximum gate bias (V_{GS} =15 V) from sample A to E is a combined result of the enhanced inverted channel mobility together with the increased electron carrier concentration (due to higher overdrive gate voltage (V_{GS}-V_{th})). Nevertheless, further reduction of the Mg concentration may lead to too low a V_{th} that may undermine the device immunity to noise signals. Our work suggests that the body doping concentration of the p-GaN layer in the vertical trench MOSFETs is a key parameter to make tradeoffs among the V_{th}, $R_{ON,sp}$ and $I_{D,max}$ in the device.

All five samples show a similar V_{th} hysteresis (ΔV_{th}) of ~1.3 V, corresponding to an interface trap density ($N_{it} = \Delta V_{th} \times C_{ox}/q$) of ~ 1×10^{12} cm^{-2}. The drain-bias-induced V_{th} shift ($\Delta V_{th}/\Delta V_{DS}$) of five samples ranges from ~90 to ~110 mV/V, as shown in TABLE I. To further investigate the gate stack properties, we have compared the measured V_{th} with theoretically predicted ones. The V_{th} can be calculated using the traditional V_{th} equation for MOSFET in the textbook [27]. Since the effective acceptor concentration (N_A) in p-GaN is different from the Mg doping concentration depending on the activation efficiency, we have extracted the N_A from test structures based on the body bias effect [27], [29], which is 3.6×, 3.1×, 2.8×, 2.2×, and 1.6 × 10^{18} cm^{-3} for sample A to E, respectively. It can be observed that the experimental V_{th} value for each sample is far lower than the theoretical value assuming no interfacial charges (Q_{it}), as shown in Fig. 6. The results suggest the existence of high-density positive interface charges in the gate stack, which may originate from residual impurities and/or dry-etching-induced N-vacancies on the p-GaN sidewall [25], [26]. Accordingly, the interface charge density ($\sigma = Q_{it}/q$) for sample A to E is estimated to be 5.1×, 4.6×, 4.5×, 4.6×, and 3.7 × 10^{12} cm^{-2}, respectively.

For the OFF-state performance, a small breakdown voltage (V_{BR}) of 60 V was initially observed in all the devices, due to an early dielectric failure at the gate-to-drain MOS junction. By employing a thick bottom dielectric in the gate trench to suppress the electric field [30], [31] without sacrificing the ON-state performance, the V_{BR} of the vertical MOSFET has been enhanced from 60 V to 273 V, close to the V_{BR} of the p-n junction of 285 V on the same epi-wafer. Details of the breakdown voltage enhancement will be reported elsewhere.

IV. Conclusion

This work reports a strong impact of p-GaN doping concentration on $R_{ON,sp}$, $I_{D,max}$, and V_{th} of vertical GaN trench MOSFETs. In a series of comparative experiments, we found that decreasing the p-GaN body doping concentration leads to an enhanced $I_{D,max}$, a lowered $R_{ON,sp}$, but also a reduced V_{th}. The p-GaN doping might be the most sensitive variable in balancing the key ON-state parameters ($R_{ON,sp}$, $I_{D,max}$, and V_{th}) in vertical GaN trench MOSFETs. From the fine tuning of Mg concentration in the p-GaN, high ON-state performance including a low $R_{ON,sp}$, a high $I_{D,max}$, a large V_{th} has been demonstrated in the quasi-vertical GaN trench MOSFET with a 2.5-μm thick drift layer maintaining a reasonable V_{BR}.

Acknowledgment

The authors thank the staff of the Nanosystem Fabrication Facility (NFF) and Material Characterization and Preparation Facility (MCPF) at HKUST for their technical support.

REFERENCES

[1] K. J. Chen, O. Häberlen, A. Lidow, C. L. Tsai, T. Ueda, Y. Uemoto, and Y. Wu, "GaN-on-Si power technology: Devices and applications," *IEEE Trans. Electron Devices*, vol. 64, no. 3, pp. 779–795, Mar. 2017, doi: 10.1109/TED.2017.2657579.

[2] M. Tao, S. Liu, B. Xie, C. P. Wen, J. Wang, Y. Hao, W. Wu, K. Cheng, B. Shen, and M. Wang, "Characterization of 880 V normally off GaN MOSHEMT on silicon substrate fabricated with a plasma-free, self-terminated gate recess process," *IEEE Trans. Electron Devices*, vol. 65, no. 4, pp. 1453–1457, Apr. 2018, doi: 10.1109/TED.2018.2808345.

[3] N. E. Posthuma, S. You, S. Stoffels, H. Liang, M. Zhao, and S. Decoutere, "Gate architecture design for enhancement mode p-GaN gate HEMTs for 200 and 650 V applications," in *Proc. IEEE 30th Int. Symp. Power Semiconductor Devices ICs (ISPSD)*, Chicago, IL, USA, May 2018, pp. 188–191, doi: 10.1109/ISPSD.2018.8393634.

[4] R. Hao, W. Li, K. Fu, G. Yu, L. Song, J. Yuan, J. Li, X. Deng, X. Zhang, Q. Zhou, Y. Fan, W. Shi, Y. Cai, X. Zhang, and B. Zhang, "Breakdown enhancement and current collapse suppression by high-resistivity GaN cap layer in normally-off AlGaN/GaN HEMTs," *IEEE Electron Device Lett.*, vol. 38, no. 11, pp. 1567–1570, Nov. 2017, doi: 10.1109/LED.2017.2749678.

[5] H. Jiang, C. W. Tang, and K. M. Lau, "Enhancement-mode GaN MOS-HEMTs with recess-free barrier engineering and high-k ZrO_2 gate dielectric," *IEEE Electron Device Lett.*, vol. 39, no. 3, pp. 405–408, Mar. 2018, doi: 10.1109/LED.2018.2792839.

[6] T. Oka, T. Ina, Y. Ueno, and J. Nishii, "1.8 mΩ·cm^2 vertical GaN-based trench metal–oxide–semiconductor field-effect transistors on a free-standing GaN substrate for 1.2-kV-class operation," *Appl. Phys. Exp.*, vol. 8, no. 5, May 2015, Art. no. 054101, doi: 10.7567/APEX.8.054101.

[7] T. Oka, T. Ina, Y. Ueno, and J. Nishii, "Over 10 a operation with switching characteristics of 1.2 kV-class vertical GaN trench MOSFETs on a bulk GaN substrate," in *Proc. 28th Int. Symp. Power Semiconductor Devices ICs (ISPSD)*, Prague, Czech Republic, Jun. 2016, pp. 459–462, doi: 10.1109/ISPSD.2016.7520877.

[8] R. Li, Y. Cao, M. Chen, and R. Chu, "600 V/1.7 Ω normally-off GaN vertical trench metal-oxide-semiconductor field-effect transistor," *IEEE Electron Device Lett.*, vol. 37, no. 11, pp. 1466–1469, Nov. 2016, doi: 10.1109/LED.2016.2614515.

[9] T. Oka, T. Ina, Y. Ueno, and J. Nishii, "100 a vertical GaN trench MOSFETs with a current distribution layer," in *Proc. 31st Int. Symp. Power Semiconductor Devices ICs (ISPSD)*, Shanghai, China, May 2019, pp. 303–306, doi: 10.1109/ISPSD.2019.8757621.

[10] C. Liu, R. A. Khadar, and E. Matioli, "GaN-on-Si quasi-vertical power MOSFETs," *IEEE Electron Device Lett.*, vol. 39, no. 1, pp. 71–74, Jan. 2018, doi: 10.1109/LED.2017.2779445.

[11] R. A. Khadar, C. Liu, R. Soleimanzadeh, and E. Matioli, "Fully vertical GaN-on-Si power MOSFETs," *IEEE Electron Device Lett.*, vol. 40, no. 3, pp. 443–446, Mar. 2019, doi: 10.1109/LED.2019.2894177.

[12] C. Gupta, S. H. Chan, Y. Enatsu, A. Agarwal, S. Keller, and U. K. Mishra, "OG-FET: An *in-situ O* xide, *G* aN interlayer-based vertical trench MOSFET," *IEEE Electron Device Lett.*, vol. 37, no. 12, pp. 1601–1604, Dec. 2016, doi: 10.1109/LED.2016.2616508.

[13] C. Gupta, C. Lund, S. H. Chan, A. Agarwal, J. Liu, Y. Enatsu, S. Keller, and U. K. Mishra, "*In situ* oxide, GaN interlayer-based vertical trench MOSFET (OG-FET) on bulk GaN substrates," *IEEE Electron Device Lett.*, vol. 38, no. 3, pp. 353–355, Mar. 2017, doi: 10.1109/LED.2017.2649599.

[14] D. Ji, C. Gupta, S. H. Chan, A. Agarwal, W. Li, S. Keller, U. K. Mishra, and S. Chowdhury, "Demonstrating >1.4 kV OG-FET performance with a novel double field-plated geometry and the successful scaling of large-area devices," in *IEDM Tech. Dig.*, San Francisco, CA, USA, Dec. 2017, pp. 9.4.1–9.4.4, doi: 10.1109/IEDM.2017.8268359.

[15] D. Ji, C. Gupta, A. Agarwal, S. H. Chan, C. Lund, W. Li, S. Keller, U. K. Mishra, and S. Chowdhury, "Large-area *in-situ* oxide, GaN interlayer-based vertical trench MOSFET (OG-FET)," *IEEE Electron Device Lett.*, vol. 39, no. 5, pp. 711–714, May 2018, doi: 10.1109/LED.2018.2813312.

[16] H. Nie, Q. Diduck, B. Alvarez, A. P. Edwards, B. M. Kayes, M. Zhang, G. Ye, T. Prunty, D. Bour, and I. C. Kizilyalli, "1.5-kV and 2.2-mΩ·cm^2 vertical GaN transistors on bulk-GaN substrates," *IEEE Electron Device Lett.*, vol. 35, no. 9, pp. 939–941, Sep. 2014, doi: 10.1109/LED.2014.2339197.

[17] D. Shibata, R. Kajitani, M. Ogawa, K. Tanaka, S. Tamura, T. Hatsuda, M. Ishida, and T. Ueda, "1.7 kV/1.0 mΩ·cm^2 normally-off vertical GaN transistor on GaN substrate with regrown p-GaN/AlGaN/GaN semipolar gate structure," in *IEDM Tech. Dig.*, San Francisco, CA, USA, Dec. 2016, pp. 10.1.1–10.1.4, doi: 10.1109/IEDM.2016.7838385.

[18] M. Sun, Y. Zhang, X. Gao, and T. Palacios, "High-performance GaN vertical fin power transistors on bulk GaN substrates," *IEEE Electron Device Lett.*, vol. 38, no. 4, pp. 509–512, Apr. 2017, doi: 10.1109/LED.2017.2670925.

[19] Y. Zhang, M. Sun, D. Piedra, J. Hu, Z. Liu, Y. Lin, X. Gao, K. Shepard, and T. Palacios, "1200 V GaN vertical fin power field-effect transistors," in *IEDM Tech. Dig.*, San Francisco, CA, USA, Dec. 2017, pp. 9.2.1–9.2.4, doi: 10.1109/IEDM.2017.8268357.

[20] Y. Zhang, M. Sun, J. Perozek, Z. Liu, A. Zubair, D. Piedra, N. Chowdhury, X. Gao, K. Shepard, and T. Palacios, "Large-area 1.2-kV GaN vertical power FinFETs with a record switching figure of merit," *IEEE Electron Device Lett.*, vol. 40, no. 1, pp. 75–78, Jan. 2019, doi: 10.1109/LED.2018.2880306.

[21] M. Kodama, M. Sugimoto, E. Hayashi, N. Soejima, O. Ishiguro, M. Kanechika, K. Itoh, H. Ueda, T. Uesugi, and T. Kachi, "GaN-based trench gate metal oxide semiconductor field-effect transistor fabricated with novel wet etching," *Appl. Phys. Exp.*, vol. 1, no. 2, Feb. 2008, Art. no. 021104, doi: 10.1143/APEX.1.021104.

[22] C. Gupta, S. H. Chan, C. Lund, A. Agarwal, O. S. Koksaldi, J. Liu, Y. Enatsu, S. Keller, and U. K. Mishra, "Comparing electrical performance of GaN trench-gate MOSFETs with a-plane $(11\bar{2}0)$ and m-plane $(1\bar{1}00)$ sidewall channels," *Appl. Phys. Exp.*, vol. 9, no. 12, Nov. 2016, Art. no. 121001, doi: 10.7567/APEX.9.121001.

[23] T. Ishida, K. P. Nam, M. Matys, T. Uesugi, J. Suda, and T. Kachi, "Improvement of channel property of GaN vertical trench MOSFET by compensating nitrogen vacancies with nitrogen plasma treatment," *Appl. Phys. Exp.*, vol. 13, no. 12, Dec. 2020, Art. no. 124003, doi: 10.35848/1882-0786/abcdbb.

[24] Y. Zhang, M. Sun, Z. Liu, D. Piedra, J. Hu, X. Gao, and T. Palacios, "Trench formation and corner rounding in vertical GaN power devices," *Appl. Phys. Lett.*, vol. 110, no. 19, May 2017, Art. no. 193506, doi: 10.1063/1.4983558.

[25] X. A. Cao, S. J. Pearton, A. P. Zhang, G. T. Dang, F. Ren, R. J. Shul, L. Zhang, R. Hickman, and J. M. Van Hove, "Electrical effects of plasma damage in p-GaN," *Appl. Phys. Lett.*, vol. 75, no. 17, pp. 2569–2571, Oct. 1999, doi: 10.1063/1.125080.

[26] D. C. Look, G. C. Farlow, P. J. Drevinsky, D. F. Bliss, and J. R. Sizelove, "On the nitrogen vacancy in GaN," *Appl. Phys. Lett.*, vol. 83, no. 17, pp. 3525–3527, Oct. 2003, doi: 10.1063/1.1623009.

[27] B. G. Streetman and S. Banerjee, *Solid State Electronic Devices*, 6th ed. Upper Saddle River, NJ, USA: Prentice-Hall, 2006.

[28] S. Takashima, K. Ueno, H. Matsuyama, T. Inamoto, M. Edo, T. Takahashi, M. Shimizu, and K. Nakagawa, "Control of the inversion-channel MOS properties by Mg doping in homoepitaxial p-GaN layers," *Appl. Phys. Exp.*, vol. 10, no. 12, Nov. 2017, Art. no. 121004, doi: 10.7567/APEX.10.121004.

[29] R. Hentschel, A. Wachowiak, A. Großer, S. Kotzea, A. Debald, H. Kalisch, A. Vescan, A. Jahn, S. Schmult, and T. Mikolajick, "Extraction of the active acceptor concentration in (pseudo-) vertical GaN MOSFETs using the body-bias effect," *Microelectron. J.*, vol. 91, pp. 42–45, Sep. 2019, doi: 10.1016/j.mejo.2019.07.011.

[30] H.-R. Chang, "Trench gate structure with thick bottom oxide," U.S. Patent 4 992 390, Feb. 12, 1991.

[31] J. D. Beasom, "Trench MOS gate device," U.S. Patent 5 770 878, Jun. 23, 1998.